

## ABSTRACT

HAMRICK, DAVID FOWLER. Investigation of Aerosol Optical Properties in the Ultraviolet Spectrum. (Under the direction of Dr. Fred Semazzi.)

Atmospheric aerosols can reduce the amount of ultraviolet (UV) radiation reaching the Earth's surface by scattering this radiation towards space and mitigating the increase of UV irradiance due to stratospheric ozone depletion. The objective of this study is to determine the amount of scattering of ultraviolet radiation by aerosol particles in the earth's atmosphere. Aerosol single scattering albedo (SSA) at UV wavelengths is an important aerosol radiative parameter in determining how aerosols affect the surface UV irradiance. An ultraviolet multi-filter rotating shadowband radiometer (UVMFR-SR) situated in Raleigh, NC, is used to gather the UV irradiances and the aerosol optical depth (AOD). These data are collected at 300 nm, 305 nm, 311 nm, 318 nm, 325 nm, 332 nm, and 368 nm. A total of 15 cloudless days were studied in the Raleigh, NC area from March to September of 2004 at a solar zenith angle of 45 degrees. The values of aerosol SSA in this study ranged from 0.68 to 0.99, with an overall average value of 0.867, indicating that aerosols are scattering most of the incident UV radiation. These results are in good agreement with previous studies. Two of these clear days were also studied for trends in SSA and black carbon levels during different times of the day. It was found that less scattering occurs during the middle of the day. A tropospheric radiative transfer model (TUV) was used to determine the SSA when values of AOD, diffuse-to-direct ratios, solar zenith angle, and time are known. The asymmetry parameter and ground albedo were given assumed values in the model, 0.70 and 0.04, respectively. The SSA values were determined by comparing the output diffuse-to-direct ratios in the model to those actually observed. More values of SSA in the ultraviolet spectrum will allow for better estimation of this parameter for future UV radiative transfer modeling and also reduce the error in estimation of surface UV irradiances.

**INVESTIGATION OF AEROSOL OPTICAL  
PROPERTIES IN THE ULTRAVIOLET SPECTRUM**

DAVID FOWLER HAMRICK

A thesis submitted to the Graduate Faculty of North Carolina State University  
in partial fulfillment of the requirements of the Degree of Master of Science

**Meteorology**

Raleigh

2005

**APPROVED BY:**

\_\_\_\_\_  
(Dr. Gary M. Lackmann)

\_\_\_\_\_  
(Dr. Sandra Yuter)

\_\_\_\_\_  
Chair of Advisory Committee

(Dr. Fred Semazzi)

\_\_\_\_\_  
(Dr. Bill Barnard)

## **Biography**

David Hamrick was born on February 6, 1980 in Jacksonville, Florida. About a year later, he and his family moved to Williamsburg, Virginia, where he was raised. Ever since the age of five, David loved the weather and climate and always knew that he wanted to be a meteorologist someday. The Weather Channel was always popular on our television set, along with the nightly weather reports on the local news. He read books on the subject even before learning about the subject in school. After spending three years of undergraduate study at Christopher Newport University in Newport News, VA, David transferred to North Carolina State University to get a Bachelor's of Science Degree in Meteorology in the spring of 2003. He then decided to continue his meteorology studies by attending the graduate program in meteorology at the same university. David's career plans include being a forecaster with the National Weather Service.

In addition to his meteorological interests, David is also very active in the autism community. Having been diagnosed with autism, he speaks at numerous autism conferences and family support groups about his experiences with growing up and living with high-functioning autism. He has served on the Board of Directors for the Commonwealth Autism Service of Virginia and also as Vice President of the Williamsburg, VA area autism society. David also loves bicycle riding and outdoor activities.

## Acknowledgements

This work was supported partially by a grant from the National Aeronautics and Space Administration and also North Carolina State University. I would like to thank Dr. Vinod K. Saxena for obtaining the funds to conduct this research. I would also like to thank my graduate committee members, Dr. Gary M. Lackmann, Dr. Frederick Semazzi, Dr. Sandra Yuter, and Dr. Bill Barnard.

Jonathan Petters and Brian Wenny have recently conducted very similar research on aerosol single scattering albedo in the ultraviolet radiation spectrum and this has provided me a background for my research on this topic. Mr. Petters deserves much credit for getting my research started and proceeding smoothly in the right direction. His work under Dr. Saxena at North Carolina State University provided much of the information necessary to conduct my research project, including the use of the TUV radiative transfer model and retrieval of the aerosol single scattering albedo. He helped me several times in properly modifying the TUV model for the Lake Wheeler research facility in Raleigh, North Carolina. He also made sure that I received the same output from the model using the Black Mountain data that he did in his own thesis to make sure the model was properly modified, before changing the settings for the Lake Wheeler site. I would still be lost in trying to configure the model code if I did not receive Mr. Petters assistance.

Dr. Bill Barnard, a recent graduate of the same university, was also extremely helpful in the collection and interpretation of the data I collected for my project at Lake Wheeler. His expertise in ultraviolet radiation and optical properties of aerosols gave me a better understanding of how aerosols act to reflect or absorb incoming solar radiation, including UV radiation. He showed me the proper way of downloading black carbon data, nephelometer data, and ozone levels at the Lake Wheeler facility. Dr. Barnard was also helpful in explaining some of the TUV radiative transfer

model concepts.

In addition, I would like to express gratitude to the staff of the USDA's UV-B Monitoring and Research Program at Colorado State University, especially John Davis, for assistance when I had questions about getting the correct data from their website regarding the diffuse-to-direct ratio (DDR) needed for the TUV model. I am particularly grateful for the availability of both DDR data and Aerosol Optical Depth data from the Lake Wheeler site and the frequent time intervals for which it was available. This definitely made my research a little easier than it would have been.

Last but not least, I want to thank my family and friends for encouraging me to move forward in my graduate studies and complete my thesis. They always thought I was capable of completing a Master's Degree, and by completing this project, I will prove that they were right.

## Table of Contents

|  | Page |
|--|------|
| List of Tables.....                                | vi   |
| List of Figures.....                               | vii  |
| Introduction.....                                  | 1    |
| Research Sites and Instrumentation.....            | 7    |
| Lake Wheeler Research Site.....                    | 7    |
| Magee Scientific Aethalometer.....                 | 8    |
| Yankee UVMFR-SR.....                               | 8    |
| Methodology.....                                   | 10   |
| Criteria for Determining Suitable Days.....        | 10   |
| Retrieval of Aerosol Single Scattering Albedo..... | 11   |
| Obtaining Black Carbon Data.....                   | 14   |
| Sensitivity Analysis.....                          | 15   |
| Results/Discussion.....                            | 16   |
| Sensitivity Analysis.....                          | 16   |
| Single Scattering Albedo Results.....              | 16   |
| Comparison of Results to Previous Studies.....     | 18   |
| Statistical Analysis.....                          | 18   |
| Discussion of Variability.....                     | 19   |
| Future Work.....                                   | 32   |
| Summary.....                                       | 33   |
| References.....                                    | 35   |

### List of Tables

|          |  |    |
|----------|--|----|
| Table 1. | Diffuse to Direct ratios of UV irradiance at the morning solar zenith angle for the 15 days studied at the Lake Wheeler UVMFR-SR site..... | 22 |
| Table 2. | Diffuse to Direct ratios at one-hour intervals during the middle of the day on April 16, 2004.....   | 22 |
| Table 3. | Diffuse to Direct ratios at one-hour intervals during the middle of the day on September 22, 2004.....                                     | 22 |
| Table 4. | Total column ozone (TOC) values gathered from the USDA's UVB Monitoring and Research Program.....  | 23 |
| Table 5. | Relative humidities, wind speed, and wind direction at Lake Wheeler for the days included in this study.....                               | 23 |
| Table 6. | Results from the sensitivity analyses on solar zenith angle, aerosol optical depth, total ozone column, and site elevation.....            | 24 |
| Table 7. | Values of single scattering albedo for each of the 15 days studied at all seven wavelengths of the UVMFR-SR.....                           | 25 |
| Table 8. | Values of single scattering albedo at one-hour intervals for April 16, 2004 and September 22, 2004.....                                    | 26 |
| Table 9. | Correlation values at the seven wavelengths between both black carbon and SSA, and between the AOD and SSA.....                            | 26 |

## List of Figures

|            |  |    |
|------------|--|----|
| Figure 1.  | Picture of the UVMFR-SR instrument used to collect ultraviolet irradiances at the USDA's Lake Wheeler site.....                    | 27 |
| Figure 2.  | Picture of the Magee Scientific Aethalometer used to measure the black carbon concentrations at Lake Wheeler.....                  | 27 |
| Figure 3.  | Estimated uncertainty in single scattering albedo as functions of wavelength and aerosol optical depth (AOD).....                  | 28 |
| Figure 4.  | Example of a plot of UV irradiances for a cloudless day as used in this study.....   | 28 |
| Figure 5.  | Example of a plot of UV irradiances for a day with considerable cloudiness.....  | 29 |
| Figure 6.  | Diagram outlining the inversion process of single scattering albedo (SSA) retrieval from the TUV radiative transfer model.....     | 29 |
| Figure 7.  | Average single scattering albedo for each UVMFR-SR wavelength for the entire study period at the 45-degree solar zenith angle..... | 30 |
| Figure 8.  | Average single scattering albedo over all seven UVMFR-SR wavelengths for each day in this study.....                               | 30 |
| Figure 9.  | Scatter plot of relative humidity measured at Lake Wheeler as a function of the single scattering albedo.....                      | 31 |
| Figure 10. | Scatter plot of wind speed measured at Lake Wheeler as a function of the single scattering albedo.....                             | 31 |

## 1. Introduction

High levels of ultraviolet (UV) radiation are harmful to animal life and agriculture. Increased levels of UV radiation, especially UV-B radiation (wavelengths of 280 nm to 320 nm), can result in higher incidences of human skin cancer, including melanoma, and cataracts. It can also suppress normal immune responses [*Madronich et al.*, 1998; *Morison*, 1989; *Taylor*, 1989]. It can cause photochemical damage to cellular structures in plant life, resulting in reduced growth, photosynthesis, and flowering abilities [*Tevini and Teramura*, 1989]. For marine life, it can result in reduced productivity and increased mortality of plants and animals near the water surface, and even affect the mobility of aquatic plankton [*Damkaer et al.*, 1981; *Bidigare*, 1989]. Increased UV radiation can lower crop production and thus threaten the food supply and raise grocery prices [*Leffell and Brash*, 1996; *Caldwell et al.*, 1986].

Stratospheric ozone levels have been gradually decreasing over recent decades, with chlorofluorocarbons (CFC's) and other ozone-destroying compounds being responsible. Minimum ozone levels of about 100 Dobson units have been observed in association with the Antarctic ozone hole during the spring months [*Stolarski et al.*, 2003]. Polar stratospheric clouds have been shown to accelerate ozone loss in localized regions of the stratosphere [*Pitari et al.*, 2002]. The presence of ozone in the stratosphere is crucial in the absorption of biologically harmful UV-B radiation. Since the discovery of the Antarctic ozone hole [*Farman et al.*, 1985], there has been a growing awareness and concern within the scientific community of the potential for increasing biological harm resulting from the destruction of stratospheric ozone [*Worrest et al.*, 1989]. There is also evidence of increasing levels of UV radiation as a result of ozone losses over the midlatitudes as well [*Bojkov and Fioletov*, 1995]. It has been predicted that a 10% stratospheric ozone reduction

will result in an estimated one million new cases of blindness from UV-induced cataracts around the world [*Krotkov et al.*, 1998].

Forecasting and warning the public about expected UV radiation levels helps people prepare before heading outdoors for an extended period of time. For example, the ultraviolet index (UVI) is a forecast tool developed by the National Weather Service to inform the general public about the health hazards of exposure to UV radiation. The UVI is the predicted noontime erythemally weighted UV irradiance in  $\text{W}/\text{m}^2$  converted to a unitless index scale. In order to issue accurate UV forecasts, realistic values of aerosol optical properties are required as inputs to improve the accuracy of UV radiative transfer modeling applications, including the UVI [*Long et al.*, 1996; *Wenny et al.*, 2001].

The United States Department of Agriculture established the UV-B Monitoring and Research Program in 1992 to address the concerns about increasing UV irradiances. The main objective of this network is to provide geographic and temporal climatology of UV irradiances for use by model developers, human health effect researchers, ecosystem scientists, and those seeking ground truth measurements for satellite measurement systems [*Bigelow et al.*, 1998]. It can also provide measurements to determine regionally representative aerosol optical depths that can be incorporated into the UVI forecast [*Wenny et al.*, 2001]. This network employs the use of Ultraviolet Multi-Filter Rotating Shadowband Radiometers (UVMFR-SR), and the data from this instrument were used to obtain the UV irradiances in this study.

The biggest factors determining UV irradiance levels at the earth's surface are the solar zenith angle, clouds, and the total column ozone. Much of the UV radiation from the sun is absorbed by the ozone layer in the stratosphere. Values of total ozone column (TOC) have been well characterized through long-term surface measurements and satellite sensing systems such as

NASA's Total Ozone Mapping Spectrometer (TOMS). Given that all other factors influencing transmission, such as clouds, aerosols, and tropospheric ozone remain constant, an increase in the surface UV irradiance is expected to follow any substantial decrease in ozone layer thickness [*Kerr and McElroy, 1993*].

Clouds and aerosols have been shown to significantly reduce the levels of UV radiation reaching the earth's surface, and also are believed to partially offset the increase of UV radiation from stratospheric ozone depletion [*Frederick et al., 1993; Meleti and Cappellani, 2000*]. Due to the high spatial and temporal variability of clouds, their effects on the exact amount of UV radiation being reflected is not well understood. Aerosols can reduce ground level UV irradiances by absorption and scattering of this radiation. These effects provide a decrease of the solar UV direct radiation, and if the aerosols are not highly absorbing, cause an increase in the diffuse component reaching the surface [*Krzyscin and Puchalski, 1998*]. *Liu et al., [1991]* recognized the importance of aerosols in the surface UV radiation balance. They estimated that the surface solar irradiance in the UV-B range had decreased over non-urban areas in the eastern United States and Europe by about 5-18% since the industrial revolution owing to increasing aerosol levels in the atmosphere. This change in aerosols had been deduced from the observed reduction in horizontal visibility.

Aerosols, such as suspended salt, dust, black carbon, and sulfate particles, have a certain albedo. This is called the aerosol single scattering albedo (SSA), which is the ratio of the scattering coefficient to the total (scattering + absorption) coefficient. The single scattering albedo can range from 0, indicating a totally absorbing aerosol, to 1, indicating a totally scattering aerosol. For the visible and UV wavelengths, this value is typically between 0.5 and 1.0, but seldom larger than 0.96, indicating that most of the incident radiation is scattered [*Lacis and Mishchenko, 1995*]. It is

an important aerosol parameter because it distinguishes between the amount of both absorbing and scattering aerosols in the atmosphere.

A type of atmospheric aerosol that has been well researched and documented in conjunction with UV radiation is black carbon. This is a pollutant that is emitted from forest fires, smoke from chimneys, and automobile exhaust, and has overall absorptive properties from its dark appearance. There are indications that black carbon and PM<sub>10</sub> have had a large impact on the UV radiation that reaches some parts of the United States, most notably the larger cities [Barnard *et al.*, 2003]. Black carbon particulates are also highly variable. The residence time of black carbon is relatively short (40 hr in rainy climates to 1 week in clean, dry regions) and controlled by several factors, such as the initial size distribution, the concentration of ambient particles, the frequency and duration of precipitation, and the efficiencies of removal mechanisms [Ogren and Charlson, 1983].

A major factor in accurately determining the SSA is the aerosol optical depth, or AOD.

Aerosol optical depth,  $\tau$ , is defined as:

$$\tau(\lambda) = \int \beta(\lambda, z) dz \quad (1)$$

where  $\beta$  is the total volume extinction (scattering + absorption) coefficient at wavelength  $\lambda$  and length  $z$  [Liu, 1980]. This parameter is determined by using the following equation:

$$\tau_{\text{total}} - \tau_{\text{rayleigh}} - \tau_{\text{ozone}} - \tau_{\text{water vapor}} = \tau_{\text{aerosol}} \quad (2)$$

where  $\tau_{\text{total}}$  is the total optical depth,  $\tau_{\text{rayleigh}}$  is the Rayleigh optical depth,  $\tau_{\text{ozone}}$  is the ozone optical depth,  $\tau_{\text{water vapor}}$  is the water vapor optical depth, and  $\tau_{\text{aerosol}}$  is the aerosol optical depth. The water vapor optical depth can be neglected because water vapor does not absorb in the UV wavelength region. It absorbs primarily in the infrared wavelength region. The Rayleigh optical depth is the contribution by air molecules. It was found that more than 80% of the aerosol effect on UV radiation due to increasing turbidity is determined by both the AOD and SSA [Reuder and

*Schwander, 1999*]. Aerosol Optical Depth is most closely related to the amount of aerosol that attenuates radiation at a specific wavelength. AOD typically varies between 0.01 and 1.00 in the UV wavelengths in a relatively clean atmosphere in a rural location, but can be higher in polluted urban air. If the AOD is above 1.0, in the case of a highly turbid atmosphere, multiple scattering of incoming radiation by aerosols becomes more significant and greatly complicates the scattering process [*Yu et al., 2000*].

To help gain a better understanding of long-term AOD trends, a 40-year study in Estonia found a potential increase of aerosol optical depth by 73% at Tõravere [*Russak, 1996*]. Ultraviolet radiation measurements analyzed with regard to aerosol impact report decreases in measured UV global irradiance by a magnitude of 25% in Barcelona, Spain [*Lorente et al., 1994*]. Another study conducted in Israel reported a 20% decrease of global irradiance during the last 40 years [*Stanhill and Janetz, 1997*]. Unfortunately, the AOD at UV wavelengths is difficult to retrieve with great accuracy due to the complicating factors of strong ozone absorption and Rayleigh scattering in the UV region, as well as the relatively large inherent uncertainty in the UV irradiance measurement over times frames of greater than 10 years [*Kerr, 1997*].

Another factor that is used to determine SSA, although to a lesser extent, is the asymmetry parameter ( $g$ ). This is an approximation of the directionality of scattering of radiation off of a particle. Asymmetry parameter,  $g$ , is defined as

$$g = 0.5 \int_{-1}^{+1} P(\Theta) \cos\Theta \, d(\cos\Theta) \quad (3)$$

where  $g = 1$  indicates complete forward scattering,  $g = -1$  indicates complete backward scattering, and  $g = 0$  indicates isotropic scattering by a particle [*Madronich and Flocke, 1997*]. For UV wavelengths,  $g$  typically falls between 0.6 and 0.8 [*Madronich, 1993*]. Ground albedo ( $g_a$ ) also plays a small role in the amount of surface UV irradiance, and it is dependent on the type of ground

surface [*Blumthaler and Ambach*, 1988; *Diffey et al.*, 1995]. A snow-covered field will reflect much more radiation than a forested region.

The main purpose of this thesis is to investigate SSA in the ultraviolet spectrum for 15 cloudless days from March to September of 2004 at a solar zenith angle of 45 degrees in the Raleigh, NC area. In addition, two of these days were chosen for hourly trends in SSA throughout the course of the day. After the SSA data had been tabulated, this was compared to the black carbon concentrations for those days to detect any possible correlation, and also correlated with the relative humidity and wind speed. There have been only limited studies of aerosol reflective properties in the ultraviolet spectrum up to this point [*Kylling et al.*, 1998; *Wenny et al.*, 1998; *Slusser et al.*, unpublished report, 2002; *Petters et al.*, 2003].

## 2. Research Sites and Instrumentation

### 2.1. Lake Wheeler Research Site

The Lake Wheeler research site is located at the United States Department of Agriculture's air quality research facility, seven miles south of downtown Raleigh, North Carolina. It is situated on a parcel of farmland owned by North Carolina State University and is about two miles from the nearest housing subdivision. This site was chosen because no previous aerosol single-scattering albedo research had been conducted at this site and it is also close to a large metropolitan area. Therefore, local pollution sources generally should be considered, especially those that involve black carbon aerosol emissions.

The site is equipped with a Yankee Environmental Systems Ultraviolet Multi-filter Rotating Shadowband Radiometer (UVMFR-SR). It is located 2 m above a grassy field at the Lake Wheeler research site and away from any building. There are no trees or other vegetation to block the sun at any time of the day except near sunrise and sunset. These devices are used by the USDA's UV-B Monitoring and Research Program at Colorado State University to study the levels of UV radiation at select sites throughout the United States and to better understand the factors which affect the level of UV radiation reaching the Earth's surface. See **Figure 1** for a picture of the UVMFR-SR at the Lake Wheeler site.

A Magee Scientific Aethalometer (**Figure 2**) was also operated at the site along with four gas instruments for monitoring ozone, sulfur dioxide, carbon monoxide, and nitrogen oxides. The aerosol sampling inlet for the Aethalometer was located approximately 2 m above the trailer's roof, with an inverted funnel at the opening. Computer hardware was also housed in the same trailer that collected and stored the data.

## 2.2. Magee Scientific Aethalometer

The aethalometer was utilized at the Lake Wheeler site throughout the entire study from March to September of 2004. Its purpose is to provide real time measurements of black carbon (BC) aerosol concentration in the lower atmosphere [*Bahrmann and Saxena, 1998; Im et al., 2001*]. The aethalometer measures the fraction of the carbonaceous aerosol that absorbs light over a broad region of the visible spectrum by determining the attenuation of light transmitted through the sample when collected on a fibrous filter [*Hansen, 1996*]. Other authors [*Gundel et al., 1984; Japar et al., 1986*] have found that optical absorption is proportional to BC concentration by the following relationship:

$$[\text{BC}] = \text{ATN}/\sigma \quad (4)$$

where ATN is the absorption coefficient (or measured absorption, in  $\text{m}^{-1}$ ), and  $\sigma$  is the specific absorption, or ATN per unit mass of BC. It has been found that the value of  $\sigma$  is dependent on a number of factors such as the origin and age of the aerosol, and whether the absorbing aerosol is internally or externally mixed with a scattering aerosol species [*Lioussse et al., 1993*]. The aethalometer uses a value of  $19 \text{ m}^2\text{g}^{-1}$ , which should be considered a first-step approximation in determining BC mass concentration.

## 2.3. Yankee Ultraviolet Multi-filter Rotating Shadowband Radiometer

The Yankee UVMFR-SR works under the same principles as the original visible wavelength version described in *Harrison et al. [1994]*. It uses seven independent interference filter photodiode detector combinations to produce total horizontal solar irradiance measurements at 300, 305.5, 311.4, 317.6, 325.4, 332.4, and 368 nm through a single Lambertian detector. An automatic, rotating shadowband, hence the instrument's name, permits the near simultaneous determination of

total, direct normal, and diffuse radiation at each of the seven wavelengths. Once the radiation is detected on the filter detectors, it is converted to voltage signals, which can then be converted back to irradiance values through the instrument's calibration equations.

Four separate measurements are taken with each pass of the shadowband. The first measurement is taken as the shadowband is at its rest (nadir) position, giving total irradiance. The other three measurements are taken with direct sunlight completely blocked from reaching the diffuser disk and one taken  $9^\circ$  to either side of the sun, giving the diffuse irradiance. These measurements allow for correction of sky area blocked by the shadowband when the sun-blocking measurement is made. Direct irradiance is computed by subtracting diffuse irradiance values from total irradiance values.

For each measurement interval, the solar position is calculated by a self-contained microprocessor. Each measurement of irradiance is corrected for the solar position and the cosine response of the instrument. The UVMFR-SR's cosine response has been laboratory tested and is accurate to within 5% for solar zenith angles between  $0$  and  $80^\circ$ .

Each of these measurements from the instrument are made sequentially at each wavelength every 20 seconds and integrated into 3-minute averages by an on-board computer system. The same computer also serves as the data logger for the UVMFR-SR. The UVMFR-SR is polled daily by a telephone modem between the field site and the UV-B Monitoring and Research Program headquarters in Fort Collins, Colorado. The database used for this study was collected between March and September of 2004 at the Lake Wheeler research facility near Raleigh, NC.

### 3. Methodology

#### 3.1. Criteria for Determining Suitable Days

Fifteen days from March to September of 2004 were examined for aerosol single scattering albedo (SSA) retrieval at the Lake Wheeler site in Raleigh, NC. In order for the day to be considered usable for SSA analysis, a sunny day with no cloud coverage was required. Another requirement was for the aerosol optical depth (AOD) at 332 nm to fall within a range of 0.14 and 0.99. A study by *Petters et al.* determined that the amount of error in SSA as a function of AOD increases exponentially as the AOD decreases, and the associated error is much greater at an AOD under 0.14. Please see **Figure 3** for a graphical depiction of SSA errors. SSA values were determined to three decimal places, with the last digit being rounded to either a 0 or a 5. Averages were not rounded.

The USDA's UV-B Monitoring and Research Program's UV irradiance plots were used to determine whether clear conditions were present for any given day. Please see **Figure 4** for a visual depiction. The seven UV irradiance graphs show smooth bell curves that correspond to the amount of solar radiation received at the surface. Any graphs that appeared asymmetrical or had major fluctuations in the irradiances were indicative of clouds and could not be used in this study. **Figure 5** is an example of a day with extensive cloud coverage. Determination of clear-sky days can also be determined with visual and infrared satellite photographs as well, but that method was not utilized in this research.

The reason why only clear days were used for SSA retrieval is that clouds complicate the transmission of UV radiation in the troposphere and greatly increase the amount of error in the UV measurements. Nonetheless, it has been shown that overcast sky conditions can attenuate up to 70% of UVB (280-320 nm) irradiance at a solar zenith angle of 50 degrees [*Schafer et al.*, 1996].

This especially holds true for deep convective clouds that extend through most of the troposphere. However, the three dimensional distribution of clouds over a region is difficult to obtain and, under the right circumstances, can increase UV irradiance reaching the surface [*Schafer et al.*, 1996; *Weihls et al.*, 2000].

The data needed for the 15 cloudless days in 2004 were downloaded from the USDA website ([http://uvb.nrel.colostate.edu/UVB/home\\_page.html](http://uvb.nrel.colostate.edu/UVB/home_page.html)) and the irradiances for a solar zenith angle of 45 degrees were selected. However, since the measurements from the UVMFR-SR were made at three-minute intervals, the reading closest to that angle was selected. These readings varied from 44.75 to 45.25 degrees and this was accounted for when running the model. These data were collected for the morning 45-degree angle for sake of consistency. A maximum of UV irradiance occurs at solar noon, but these were not used in the study since the maximum solar zenith angle is not the same for each day. This angle was chosen as a fixed variable so that the rays of the sun maintained a constant path length through the atmosphere, allowing for fewer variables to be analyzed. This was also the reason why the time period from March to September was used since these months had higher sun angles than October through February.

### **3.2. Retrieval of Aerosol Single Scattering Albedo**

At the 45-degree solar zenith angle, both the direct and diffuse UV irradiances were collected to determine the direct-to-diffuse ratio (DDR) for the seven operational wavelengths of the UVMFR-SR. **Table 1** shows the DDR values for each of the 15 days used in this study, and **Tables 2 and 3** show the DDR for the days with hourly SSA retrievals. The total irradiance is the amount of UV light reaching the sensor of the UVMFR-SR instrument without any shade. The diffuse

irradiance is the amount reaching the sensor with the shadowband blocking the direct rays of the sun. The direct irradiance is obtained by subtracting the diffuse irradiance from the total irradiance.

An iterative procedure was used to determine the SSA in the TUV model. **Figure 6** shows a flow chart of how this process works. The model inputs relative to this study are the latitude, longitude, solar zenith angle, date of measurement, aerosol optical depth (AOD), total ozone column (TOC), ground albedo (ga), asymmetry parameter (g), and the single scattering albedo (SSA). The outputs of the model are the DDR values at the seven operational wavelengths of the UVMFR-SR. Reasonable guesses of SSA are made to output the DDR values. The objective here is to get the model's output of the DDR as close to the observed value of DDR at a given wavelength when making educated guesses of the SSA. While trying to determine the SSA by matching the DDR values, the AOD values were kept constant. The same model was also used at the Black Mountain UVMFR-SR site in western North Carolina to retrieve SSA in previous studies [*Wenny et al.*, 1998; *Petters et al.*, 2003].

In addition to determining the DDR, the aerosol optical depth (AOD) was also downloaded from the UVB Monitoring and Research Program. The AOD was available as three-minute averages at both the 332 nm and 368 nm wavelengths. The value of the AOD for the three-minute period corresponding to the same time as the 45-degree solar zenith angle was used as input in the TUV radiative transfer model. Total optical depths (TOD) are calculated using the standard Beer's Law approach:

$$\text{TOD} = \frac{\ln(V_0) - \ln(V)}{\text{airmass}} \quad (5)$$

where the airmass is simply the secant of the solar zenith angle and  $V_0$  is the voltage signal the UVMFR-SR would record at the top of the atmosphere. Rayleigh and ozone optical depths are subtracted from the total optical depth (TOD) to yield the aerosol optical depths. The contribution

by water vapor and other trace gases is insignificant to the outcome of the AOD, so it can be neglected in this approximation.  $V_0$  for each wavelength and specific time is determined from a time series of Langley-generated voltage intercepts for morning periods. The Langley method is described in *Harrison and Michalsky, 1994*.

The AOD values at 332 nm were used in this study. A large degree of uncertainty exists for AOD values at the lower wavelengths and the AOD for 368 nm would have been a less representative value for the UV spectrum, therefore the 332 values were best. A previous study used AOD at 340 nm in determining SSA at Black Mountain, NC [*Petters et al., 2003*]. They also used AOD as averages for the entire period when the solar zenith angle was less than 60 degrees, whereas this study used instantaneous values. The TUV model assumes that AOD varies inversely with the first power of wavelength [*Madronich, 1993*], and that it varies with altitude according to the *Elterman* [1968] profile.

Total ozone column (TOC) measurements were also provided by the UVB Monitoring and Research Program. These values were calculated by the direct-sun method [*Gao et al., 2001*]. The direct-sun total column ozone retrievals are made with the UVMFR-SR by measurement of the relative intensities of selected pairs of UV wavelengths, as with the Dobson spectrophotometer [*Komhyr, 1980*]. Please see **Table 4** for all of the TOC readings.

Asymmetry parameter,  $g$ , was assumed a value of 0.70, for all wavelengths and altitudes, since this is the average value as determined by *Madronich, 1993*. Ground albedo,  $g_a$ , was assumed a value of 0.04, for all wavelengths and altitudes. This value was originally taken from *Schwander et al.* [1997]. These two parameters play a smaller role in the determination of SSA than the AOD and DDR.

The TUV model is also modified for the site location and elevation. In this case, the Lake Wheeler elevation is 124 m ASL and located at 35.72°N latitude and 78.68°W longitude. These values are important because this tells the model where the station is geographically located and the elevation provides information about the vertical depth of the atmosphere that the rays of the sun must penetrate before reaching the surface. The amount of incoming UV radiation is much higher at greater altitudes since the radiation from the sun has less depth of the atmosphere to penetrate.

The same methods were used for April 16, 2004 and September 22, 2004, when hourly measurements were collected to examine how the SSA varies throughout a given day at different solar zenith angles. For both of these days, data were collected at the following UTC times: 1400, 1500, 1600, 1700, 1800, 1900, 2000, and 2100 hrs. These times correspond to the times 10:00 am through 5:00 pm eastern daylight time at the Lake Wheeler site. During the period of daylight before and after these times, the solar zenith angle was too low and this complicated the DDR values, thus limiting the amount of time for SSA retrieval to the middle part of the day. The lower solar elevation angles shortly after sunrise and shortly before sunset also result in longer penetration of the sun's radiation into the atmosphere, thus complicating the scattering process.

Relative humidities taken at the Lake Wheeler site were compiled for the hour closest to the SSA retrieval time to determine whether it had any significant effect on the SSA. These data were collected for only the 45-degree solar zenith angle. An average relative humidity of 41.6% was found over the 15-day study period, with two days missing data (**Table 5**). Large relative humidities, greater than 70%, have been shown to increase the aerosol scattering in the visible wavelengths and also yield a higher SSA [*Waggoner et al.*, 1981]. In this study, each of the days had RH values less than 70%.

### 3.3. Obtaining Black Carbon Data

Another goal of this research is to determine the correlation between black carbon concentrations in the lower atmosphere to the aerosol single scattering albedo. These concentrations in the environment were measured using the aethalometer housed in a trailer on site. This instrument records the ambient black carbon concentration ( $\text{ng}/\text{m}^3$ ) every fifteen minutes and records this information onto a disk. Once downloaded, the data were quality controlled to check that the flow rate was near 5 liters per minute and that there were either no extreme outliers in the data nor any negative numbers that were erroneously reported. The black carbon reading that was closest in time to the 45-degree solar zenith angle was used. The same holds true for the data taken to determine hourly trends in SSA. Measurements three hours before and after these times were examined for consistency, and if there were erratic patterns or sudden increases or decreases near the time of the observation, that day was not considered good for SSA analysis. This includes those days for which black carbon data was unavailable. Therefore, several clear days had to be rejected

### 3.4. Sensitivity Analysis

It is necessary to perform sensitivity studies so that error in this technique to retrieve SSA can be determined. Four different tests were conducted to see which input played the greatest role in determining DDR. One parameter was varied holding the others constant. The analyses done were changing the solar zenith angle from 44.77 to 49.77 degrees, doubling the altitude of the site from 124m to 248m, raising the AOD from 0.235 to 0.335, and lowering the TOC from 349.5 DU to 249.5 DU. The resulting changes in DDR values would be proportional to the changes in the SSA values. The asymmetry parameter ( $g=0.70$ ) and the ground albedo ( $g_a=0.04$ ) were kept constant throughout all of these runs.

## 4. Results/Discussion

### 4.1. Sensitivity Analysis

**Tables 6.1 – 6.4** show the results of the sensitivity analysis. The first test was to determine the amount of change in the diffuse-to-direct ratio (DDR) when the solar zenith angle is increased by five degrees, from  $44.77^\circ$  to  $49.77^\circ$ . This change resulted in a 9.13% increase in the overall DDR values. Raising the AOD from 0.235 to 0.335 proved to cause the biggest overall change in the DDR, with an increase of 15.19%. Decreasing the total ozone column by 100 DU, from 349.5 DU to 249.5, was less significant with an overall DDR increase of just 1.97%. Finally, doubling the elevation of the UVMFR-SR site from 124 m to 248 m also had a small effect on the DDR values. This actually resulted in a small 1.78% decrease in the DDR. The changes in the DDR values as a result of changing these variables would be proportional to the changes in the single scattering albedo. Therefore, the solar zenith angle and aerosol optical depth are the biggest factors in determining the DDR and the single scattering albedo.

### 4.2. Single Scattering Albedo Results

Single scattering albedo (SSA) values were obtained for the seven wavelengths of the UV-MFRSR for 15 days from March 11 to September 23 of 2004 at a solar zenith angle of 45 degrees. The value of SSA ranged from 0.680 - 0.925 at 300 nm, 0.710 - 0.930 at 305.5 nm, 0.755 – 0.960 at 311.4 nm, 0.755 – 0.960 at 317.6 nm, 0.760 – 0.970 at 325.4 nm, 0.755 – 0.975 at 332.4 nm, and 0.715 – 0.990 at 368 nm (**Figure 7**). The mean values of SSA were 0.835 at 300 nm, 0.853 at 305.5 nm, 0.879 at 311.4 nm, 0.879 at 317.6 nm, 0.882 at 325.4 nm, 0.881 at 332.4 nm, and 0.858 at 368 nm. **Figure 8** shows the daily SSA averages for all 15 days. The overall average SSA for all the wavelengths was 0.867. **Table 7** shows the days that were analyzed in this study along with the

SSA results at the seven different wavelengths of the UVMFR-SR. These values are close to what other studies have found [*Petters et al.*, 2003; *Wenny et al.*, 1998].

SSA values were also computed for both April 16 and September 22, 2004 at eight different times during the day. The first time was at 1400 UTC (10:00 am EDT) and then for each hour after that until 2100 UTC (5:00 pm EDT). These data are shown in **table 8**. These were the times closest to the maximum solar zenith angle for the day, all with clear sky conditions present. The highest SSA was found to occur at the beginning and end of these hourly periods, with the lowest SSA during the middle of the day. In other words, the shorter path length of the sun's radiation through the atmosphere around midday resulted in less scattering. This was found to hold true for all wavelengths of the UVMFR-SR. The overall SSA for April 16 for all eight tabulations was 0.7039 and the overall SSA for September 22 was considerably higher at 0.9424. The higher relative humidity on the latter day may be responsible for the greater SSA values, and possibly because of a greater presence of sulfate aerosols in the atmosphere.

**Tables 1 - 3** display the values of DDR measured by the UVMFR-SR that were matched as output from TUV4.1. The DDR values were greatest at 300 nm and decreased with greater wavelengths, with the greatest change from 332.4 nm to 368 nm. Therefore, there is more diffuse radiation at the shorter wavelengths of the UV spectrum. A maximum DDR value of 4.892 was observed on May 22, 2004 at 300 nm. A minimum DDR value of 0.544 was observed on May 6, 2004 at 368 nm. A similar behavior of DDR values was observed for both April 16, 2004 and September 22, 2004 when hourly values were tabulated. DDR can be expected to vary widely with aerosol optical depth, size distribution, shape, and chemical composition, as with other radiative properties. In addition, Rayleigh scattering is greater at smaller wavelengths, particularly below 311 nm.

### 4.3. Comparison of Results to Previous Studies

The values of aerosol single scattering albedo in this study ranged from 0.68 to 0.99, with an overall average value of 0.867, at Lake Wheeler, with the aerosol optical depth (AOD) measurements at 332.4 nm. As a point of reference for previous studies, the range at 311.4 nm was 0.755 to 0.960. These results fall within the ranges reported by other SSA studies in the past decade, with no extreme outliers in the data. *Wenny et al.* [1998] determined SSA for nine days in 1995 at 311.4 nm at Black Mountain, NC. His values of SSA ranged from 0.75 - 0.93, with an average of 0.834. There was no discernible dependence on air mass type. However, due to some of those days having relative humidities at or above 80%, higher SSA values can be expected. This range of values is slightly smaller than the values presented in the *Petters et al.* [2003] study, also at Black Mountain, which ranged from 0.73 – 0.97 at 311.4 nm. The *Petters et al.* study noted an overall range of SSA from a minimum of 0.65 at 300 nm to a maximum of 0.99 at 368 nm, with the AOD value at 340 nm being used. The overall average SSA in that study was 0.870. Another study, by *Kylling et al.* [1998], found a range of SSA between 0.83 and 0.99 when they conducted an ultraviolet radiation study in Greece during June of 1996. Unlike later studies, the value of SSA was assumed to be independent of wavelength. They matched spectral UV irradiance from two spectroradiometers with a radiative transfer model that uses a discrete ordinate algorithm, similar to the model employed in this study.

### 4.4. Statistical Analysis

The correlation between SSA and black carbon concentrations measured by the aethalometer at the Lake Wheeler site was investigated in this study. Surprisingly, only a weak correlation was found between these two values for all seven wavelengths, including the average SSA values. For

the 300 nm and 305 nm wavelengths, a 0.029 and 0.021 correlation, respectively, was found. For the other five wavelengths, a small negative correlation was found. The overall average correlation over all wavelengths was -0.028, meaning that lower levels of black carbon aerosols increased the SSA of aerosols in the ultraviolet spectrum, but to a very limited extent. It is possible that the black carbon concentrations were too small to have a significant effect on the SSA. These correlation values were determined using Microsoft Excel software by the following formula:

$$\text{Correl}(X, Y) = \frac{\sum (x - \bar{x})(y - \bar{y})}{\sqrt{\sum (x - \bar{x})^2 \sum (y - \bar{y})^2}} \quad (6)$$

where X is the black carbon concentration array and Y is the SSA array. The same formula was applied to determine the correlation between the AOD at 332.4 nm and the single scattering albedo. In contrast to the black carbon, there was a strong positive correlation of 0.5915, with the greatest correlation of 0.689 at 368 nm and the lowest at 311.4 nm. Therefore, the SSA is generally higher on days when the AOD is highest. Please see **Table 9** for all of these results.

#### 4.5. Discussion of Variability

In this paper, the average SSA over all seven wavelengths varied from a minimum of 0.735 on May 6, 2004, to a maximum of 0.956 on August 19, 2004. The standard deviation for these data was 0.071. Since black carbon did not show a strong correlation signal with the SSA values retrieved for this study, it was necessary to investigate a few other meteorological parameters from the Lake Wheeler research site to ascertain why the SSA varied. Hourly measurements of wind speed, wind direction, and relative humidity from the site via the North Carolina State Climate Office's NC CRONOS database were obtained nearest the time of the morning 45-degree solar

zenith angle and at a height of 2 meters above the ground, the same height as the UVMFR-SR. See **Table 5** for these results.

In the *Petters et al.* [2003] study, SSA values were correlated with air mass origin to see if there was a significant relationship. Three different air mass sectors were identified: marine, continental, and highly polluted, with the latter being from the Ohio Valley area and the northeastern United States. No significant dependence on air mass type was identified in that study, nor in the *Wenny et al.* [1998] study. This can be attributed to the widely varying aerosol content of air masses coming from each sector. The highly polluted sector is dominated by the highest concentration of soot and sulfate aerosols [*Deininger and Saxena*, 1997]. Sulfate particles form in the air from sulfur dioxide gas. Most of this gas is released from coal-burning power plants and other industrial sources, such as smelters, industrial boilers, and oil refineries. Sulfates are the largest contributor to haze in the eastern United States, due to the large number of coal-fired power plants that affect the region [Malm, 1999]. In humid environments, sulfate particles grow rapidly to a size that is very efficient at scattering light.

Examining the Lake Wheeler data, a positive correlation of 0.664 was found between the relative humidity and the single scattering albedo. Therefore, the SSA generally increased as the relative humidity increased (**Figure 9**). The linear regression equation that best represents these results is:

$$y = 103.11x - 47.05 \quad (7)$$

This is consistent with the finding by *Waggoner et al.* [1981], even though the RH never exceeded 70% in this study. This relationship between the relative humidity and single scattering albedo can be explained via the chemical properties of aerosols. Aerosols often contain chemical species, such as inorganic ions (sulfate, nitrate, ammonium, etc.), that are hygroscopic [*Charlson et al.*, 1974;

*Tang, 1980; Rood et al., 1987*]. When present, these species take on water with increasing relative humidity, resulting in an increase in light scattering. The change in light scattering with RH depends on the chemical composition of the aerosol as well as the dry size distribution [*McInnes et al., 1998*].

In addition, higher values of SSA were noted with winds from the west and southwest directions, indicative of a continental air mass. Sulfate aerosols are likely responsible for the higher SSA values observed as they are whitish in appearance, thus making them better at scattering solar radiation. A fairly small, positive correlation of 0.453 was found when comparing wind speed measurements with the SSA. Therefore, there was a slight decrease in SSA with lower wind speeds at the site (**Figure 10**). On April 16, 2004, an SSA of 0.736 was found with a wind of 0.1 mph as measured at Lake Wheeler. The generally higher SSA values with greater winds may be explained by the wind picking up more dust particles from the ground and spreading smoke and emissions from industrial sources, thus increasing the number of aerosols in the air. With lighter wind speeds in a semi-rural area, such as Lake Wheeler, more particles are able to fall out of the air and there is less advection of particulates from distant sources.

Table 1. Diffuse to Direct ratios of UV irradiance at the morning solar zenith angle for the 15 days studied at the Lake Wheeler UVMFR-SR site.

| Date           | DDR 300      | DDR 305      | DDR 311      | DDR 317      | DDR 325      | DDR 332      | DDR 368      |
|----------------|--------------|--------------|--------------|--------------|--------------|--------------|--------------|
| 3/11/2004      | 1.295        | 1.300        | 1.270        | 1.162        | 1.041        | 0.916        | 0.545        |
| 3/20/2004      | 1.666        | 1.584        | 1.536        | 1.423        | 1.274        | 1.152        | 0.683        |
| 4/9/2004       | 1.657        | 1.640        | 1.607        | 1.485        | 1.341        | 1.222        | 0.733        |
| 4/16/2004      | 1.309        | 1.303        | 1.277        | 1.197        | 1.073        | 0.964        | 0.566        |
| 4/17/2004      | 1.990        | 1.975        | 1.907        | 1.791        | 1.606        | 1.439        | 0.846        |
| 4/23/2004      | 1.977        | 1.958        | 1.885        | 1.770        | 1.573        | 1.417        | 0.859        |
| 5/4/2004       | 1.330        | 1.322        | 1.278        | 1.198        | 1.077        | 0.969        | 0.575        |
| 5/6/2004       | 1.301        | 1.291        | 1.254        | 1.167        | 1.044        | 0.935        | 0.544        |
| 5/21/2004      | 2.709        | 2.678        | 2.541        | 2.383        | 2.160        | 1.946        | 1.235        |
| 5/22/2004      | 4.892        | 4.746        | 4.540        | 4.308        | 3.908        | 3.592        | 2.309        |
| 6/20/2004      | 2.316        | 2.294        | 2.190        | 2.044        | 1.836        | 1.656        | 1.037        |
| 8/19/2004      | 3.562        | 3.579        | 3.501        | 3.324        | 3.042        | 2.792        | 1.864        |
| 8/20/2004      | 4.739        | 4.678        | 4.599        | 4.427        | 4.034        | 3.753        | 2.494        |
| 9/22/2004      | 1.548        | 1.524        | 1.460        | 1.345        | 1.199        | 1.072        | 0.632        |
| 9/23/2004      | 1.635        | 1.621        | 1.554        | 1.438        | 1.272        | 1.139        | 0.651        |
| <b>Average</b> | <b>2.262</b> | <b>2.233</b> | <b>2.160</b> | <b>2.031</b> | <b>1.832</b> | <b>1.664</b> | <b>1.038</b> |

Table 2. Diffuse to Direct ratios at one-hour intervals during the middle of the day on April 16, 2004

| UTC Time       | DDR 300      | DDR 305      | DDR 311      | DDR 318      | DDR 325      | DDR 332      | DDR 368      |
|----------------|--------------|--------------|--------------|--------------|--------------|--------------|--------------|
| 14:00:00       | 1.635        | 1.509        | 1.452        | 1.346        | 1.188        | 1.058        | 0.602        |
| 15:00:00       | 1.183        | 1.200        | 1.183        | 1.123        | 1.016        | 0.912        | 0.548        |
| 16:00:00       | 1.077        | 1.107        | 1.098        | 1.043        | 0.951        | 0.867        | 0.533        |
| 17:00:00       | 1.019        | 1.058        | 1.054        | 1.004        | 0.915        | 0.835        | 0.519        |
| 18:00:00       | 1.052        | 1.094        | 1.086        | 1.037        | 0.948        | 0.862        | 0.537        |
| 19:00:00       | 1.163        | 1.202        | 1.187        | 1.124        | 1.024        | 0.926        | 0.572        |
| 20:00:00       | 1.395        | 1.401        | 1.347        | 1.258        | 1.135        | 1.020        | 0.602        |
| 21:00:00       | 2.050        | 2.034        | 1.857        | 1.625        | 1.429        | 1.260        | 0.688        |
| <b>Average</b> | <b>1.322</b> | <b>1.326</b> | <b>1.283</b> | <b>1.195</b> | <b>1.076</b> | <b>0.968</b> | <b>0.575</b> |

Table 3. Diffuse to Direct ratios at one-hour intervals during the middle of the day on Sept. 22, 2004.

| UTC Time       | DDR 300      | DDR 305      | DDR 311      | DDR 317      | DDR 325      | DDR 332      | DDR 368      |
|----------------|--------------|--------------|--------------|--------------|--------------|--------------|--------------|
| 14:00:00       | 2.387        | 2.137        | 1.947        | 1.754        | 1.504        | 1.325        | 0.722        |
| 15:00:00       | 1.595        | 1.577        | 1.500        | 1.379        | 1.225        | 1.100        | 0.644        |
| 16:00:00       | 1.380        | 1.382        | 1.343        | 1.248        | 1.116        | 1.006        | 0.605        |
| 17:00:00       | 1.296        | 1.309        | 1.268        | 1.187        | 1.064        | 0.966        | 0.584        |
| 18:00:00       | 1.340        | 1.348        | 1.301        | 1.215        | 1.086        | 0.980        | 0.588        |
| 19:00:00       | 1.484        | 1.482        | 1.410        | 1.307        | 1.163        | 1.038        | 0.608        |
| 20:00:00       | 1.979        | 1.877        | 1.734        | 1.566        | 1.371        | 1.204        | 0.666        |
| 21:00:00       | 5.667        | 3.453        | 2.741        | 2.323        | 1.947        | 1.641        | 0.792        |
| <b>Average</b> | <b>2.141</b> | <b>1.821</b> | <b>1.656</b> | <b>1.497</b> | <b>1.310</b> | <b>1.157</b> | <b>0.651</b> |

Table 4. Total column ozone (TOC) values gathered from the USDA's UVB Monitoring and Research Program, using the direct-sun method. These values are expressed in Dobson units.

| Date           | Ozone        |
|----------------|--------------|
| 3/11/2004      | 269.8        |
| 3/20/2004      | 295.0        |
| 4/9/2004       | 294.5        |
| 4/16/2004      | 349.5        |
| 4/17/2004      | 361.3        |
| 4/23/2004      | 304.7        |
| 5/4/2004       | 344.7        |
| 5/6/2004       | 333.7        |
| 5/21/2004      | 322.5        |
| 5/22/2004      | 324.1        |
| 6/20/2004      | 292.6        |
| 8/19/2004      | 299.5        |
| 8/20/2004      | 292.3        |
| 9/22/2004      | 268.5        |
| 9/23/2004      | 280.2        |
| <b>Average</b> | <b>309.5</b> |

Table 5. Values of relative humidity, wind speed, and direction from the Lake Wheeler site at the time of the morning solar zenith angle. MM refers to missing data. Data courtesy of the State Climate Office of North Carolina.

| Date           | Overall SSA  | RH %        | Speed mph  | Direction | Degrees |
|----------------|--------------|-------------|------------|-----------|---------|
| 3/11/2004      | 0.914        | 37          | 16.5       | WNW       | 289     |
| 3/20/2004      | 0.892        | 47          | 9.5        | WSW       | 242     |
| 4/9/2004       | 0.868        | MM          | MM         | MM        | MM      |
| 4/16/2004      | 0.736        | 25          | 0.1        | WNW       | 288     |
| 4/17/2004      | 0.828        | 34          | 6.7        | SW        | 221     |
| 4/23/2004      | 0.858        | 45          | 11.7       | WSW       | 252     |
| 5/4/2004       | 0.747        | 39          | 5.8        | WNW       | 288     |
| 5/6/2004       | 0.735        | 31          | 5.8        | N         | 0       |
| 5/21/2004      | 0.909        | 51          | 6.7        | WSW       | 243     |
| 5/22/2004      | 0.936        | 64          | 9.2        | WSW       | 242     |
| 6/20/2004      | 0.897        | 32          | 8          | E         | 100     |
| 8/19/2004      | 0.956        | MM          | MM         |           | MM      |
| 8/20/2004      | 0.939        | 60          | 9.2        | SW        | 237     |
| 9/22/2004      | 0.89         | 33          | 0.7        | ENE       | 72      |
| 9/23/2004      | 0.898        | 43          | 3.6        | N         | 5       |
| <b>Average</b> | <b>0.867</b> | <b>41.6</b> | <b>7.2</b> |           |         |

Table 6.1. Sensitivity of DDR values to changing the solar zenith angle from 44.77° to 49.77°

| $\lambda$      | Z = 44.77° | Z = 49.77° | Change          | Percent     |
|----------------|------------|------------|-----------------|-------------|
| 300.0          | 1.30873    | 1.50643    | 0.19770         | 15.11       |
| 305.5          | 1.30300    | 1.45209    | 0.14909         | 11.44       |
| 311.4          | 1.27685    | 1.40217    | 0.12532         | 9.81        |
| 317.6          | 1.19661    | 1.30071    | 0.10410         | 8.70        |
| 325.4          | 1.07295    | 1.15534    | 0.08239         | 7.68        |
| 332.4          | 0.96424    | 1.03068    | 0.06644         | 6.89        |
| 368.0          | 0.56637    | 0.59051    | 0.02414         | 4.26        |
| <b>Average</b> |            |            | <b>0.107026</b> | <b>9.13</b> |

Table 6.2. Sensitivity of DDR values to changing the AOD from 0.235 to 0.335

| $\lambda$      | AOD = 0.235 | AOD = 0.335 | Change          | Percent      |
|----------------|-------------|-------------|-----------------|--------------|
| 300.0          | 1.30873     | 1.48811     | 0.17938         | 13.71        |
| 305.5          | 1.30300     | 1.48403     | 0.18103         | 13.89        |
| 311.4          | 1.27685     | 1.46813     | 0.19128         | 14.98        |
| 317.6          | 1.19661     | 1.37744     | 0.18083         | 15.11        |
| 325.4          | 1.07295     | 1.23783     | 0.16488         | 15.37        |
| 332.4          | 0.96424     | 1.11588     | 0.15164         | 15.73        |
| 368.0          | 0.56637     | 0.66592     | 0.09955         | 17.58        |
| <b>Average</b> |             |             | <b>0.164084</b> | <b>15.19</b> |

Table 6.3. Sensitivity of DDR values to lowering the TOC from 349.5 DU to 249.5 DU.

| $\lambda$      | TOC = 349.5 | TOC = 249.5 | Change          | Percent     |
|----------------|-------------|-------------|-----------------|-------------|
| 300.0          | 1.30873     | 1.37156     | 0.06283         | 4.80        |
| 305.5          | 1.30300     | 1.35196     | 0.04896         | 3.76        |
| 311.4          | 1.27685     | 1.31064     | 0.03379         | 2.65        |
| 317.6          | 1.19661     | 1.21536     | 0.01875         | 1.57        |
| 325.4          | 1.07295     | 1.08139     | 0.00844         | 0.79        |
| 332.4          | 0.96424     | 0.96566     | 0.00142         | 0.15        |
| 368.0          | 0.56637     | 0.56693     | 0.00056         | 0.10        |
| <b>Average</b> |             |             | <b>0.024964</b> | <b>1.97</b> |

Table 6.4. Sensitivity of DDR values to doubling the site elevation from 124 m to 248 m.

| $\lambda$      | H = 124 m | H = 248 m | Change          | Percent      |
|----------------|-----------|-----------|-----------------|--------------|
| 300.0          | 1.30873   | 1.28449   | -0.02424        | -1.85        |
| 305.5          | 1.30300   | 1.27697   | -0.02603        | -2.00        |
| 311.4          | 1.27685   | 1.25269   | -0.02416        | -1.89        |
| 317.6          | 1.19661   | 1.17385   | -0.02276        | -1.90        |
| 325.4          | 1.07295   | 1.05342   | -0.01953        | -1.82        |
| 332.4          | 0.96424   | 0.94764   | -0.01660        | -1.72        |
| 368.0          | 0.56637   | 0.55909   | -0.00728        | -1.29        |
| <b>Average</b> |           |           | <b>-0.02009</b> | <b>-1.78</b> |

Table 7. Values of single scattering albedo for each of the 15 days studied at all seven wavelengths of the UVMFR-SR. This information is taken with the AOD at 332 nm. The black carbon concentration at the time of the 45-degree solar zenith angle is also noted here.

| Date            | BC<br>(ng)    | 332<br>AOD   | 300<br>SSA   | 305<br>SSA   | 311<br>SSA   | 317<br>SSA   | 325<br>SSA   | 332<br>SSA   | 368<br>SSA   | Average<br>SSA |
|-----------------|---------------|--------------|--------------|--------------|--------------|--------------|--------------|--------------|--------------|----------------|
| 3/11/2004       | 227.50        | 0.149        | 0.815        | 0.890        | 0.960        | 0.935        | 0.950        | 0.920        | 0.930        | 0.914          |
| 3/20/2004       | 244.75        | 0.275        | 0.910        | 0.875        | 0.900        | 0.895        | 0.895        | 0.905        | 0.865        | 0.892          |
| 4/9/2004        | 328.00        | 0.310        | 0.825        | 0.845        | 0.880        | 0.875        | 0.885        | 0.900        | 0.865        | 0.868          |
| 4/16/2004       | 366.50        | 0.235        | 0.680        | 0.710        | 0.755        | 0.760        | 0.760        | 0.760        | 0.725        | 0.736          |
| 4/17/2004       | 336.75        | 0.453        | 0.815        | 0.835        | 0.845        | 0.850        | 0.840        | 0.835        | 0.775        | 0.828          |
| 4/23/2004       | 257.50        | 0.422        | 0.840        | 0.855        | 0.870        | 0.875        | 0.875        | 0.860        | 0.830        | 0.858          |
| 5/4/2004        | 259.00        | 0.233        | 0.700        | 0.730        | 0.755        | 0.760        | 0.770        | 0.770        | 0.745        | 0.747          |
| 5/6/2004        | 670.00        | 0.213        | 0.685        | 0.720        | 0.755        | 0.755        | 0.760        | 0.755        | 0.715        | 0.735          |
| 5/21/2004       | 711.00        | 0.587        | 0.900        | 0.910        | 0.910        | 0.910        | 0.915        | 0.910        | 0.910        | 0.909          |
| 5/22/2004       | 328.50        | 0.960        | 0.925        | 0.925        | 0.930        | 0.935        | 0.940        | 0.945        | 0.950        | 0.936          |
| 6/20/2004       | 187.00        | 0.506        | 0.855        | 0.870        | 0.910        | 0.910        | 0.915        | 0.910        | 0.910        | 0.897          |
| 8/19/2004       | 375.75        | 0.749        | 0.915        | 0.930        | 0.950        | 0.960        | 0.970        | 0.975        | 0.990        | 0.956          |
| 8/20/2004       | 582.50        | 0.955        | 0.900        | 0.905        | 0.925        | 0.940        | 0.950        | 0.965        | 0.985        | 0.939          |
| 9/22/2004       | 499.50        | 0.236        | 0.875        | 0.890        | 0.910        | 0.900        | 0.900        | 0.895        | 0.860        | 0.890          |
| 9/23/2004       | 496.50        | 0.268        | 0.890        | 0.910        | 0.930        | 0.920        | 0.910        | 0.905        | 0.820        | 0.898          |
| <b>Averages</b> | <b>391.38</b> | <b>0.437</b> | <b>0.835</b> | <b>0.853</b> | <b>0.879</b> | <b>0.879</b> | <b>0.882</b> | <b>0.881</b> | <b>0.858</b> | <b>0.867</b>   |

Table 8. Values of single scattering albedo, along with AOD values and black carbon concentration at one-hour intervals for April 16, 2004, and the second chart for September 22, 2004.

| UTC Time       | AOD 332       | BC data        | SSA 300       | SSA 305       | SSA 311       | SSA 318       | SSA 325       | SSA 332       | SSA 368       | Average       |
|----------------|---------------|----------------|---------------|---------------|---------------|---------------|---------------|---------------|---------------|---------------|
| 14:00:00       | 0.243         | 362            | 0.720         | 0.700         | 0.745         | 0.755         | 0.750         | 0.755         | 0.710         | 0.734         |
| 15:00:00       | 0.256         | 395            | 0.635         | 0.665         | 0.705         | 0.720         | 0.720         | 0.715         | 0.680         | 0.691         |
| 16:00:00       | 0.274         | 311            | 0.645         | 0.665         | 0.695         | 0.700         | 0.700         | 0.700         | 0.665         | 0.681         |
| 17:00:00       | 0.270         | 381            | 0.640         | 0.660         | 0.690         | 0.695         | 0.695         | 0.690         | 0.660         | 0.676         |
| 18:00:00       | 0.280         | 330            | 0.650         | 0.680         | 0.700         | 0.710         | 0.710         | 0.710         | 0.670         | 0.690         |
| 19:00:00       | 0.295         | 311            | 0.660         | 0.695         | 0.720         | 0.720         | 0.725         | 0.720         | 0.690         | 0.704         |
| 20:00:00       | 0.285         | 236            | 0.670         | 0.715         | 0.730         | 0.730         | 0.740         | 0.740         | 0.700         | 0.718         |
| 21:00:00       | 0.277         | 203            | 0.670         | 0.765         | 0.780         | 0.735         | 0.745         | 0.750         | 0.715         | 0.737         |
| <b>Average</b> | <b>0.2730</b> | <b>316.125</b> | <b>0.6613</b> | <b>0.6931</b> | <b>0.7206</b> | <b>0.7206</b> | <b>0.7231</b> | <b>0.7225</b> | <b>0.6863</b> | <b>0.7039</b> |

| UTC Time       | AOD 332       | BC data        | SSA 300       | SSA 305       | SSA 311       | SSA 317       | SSA 325       | SSA 332       | SSA 368       | Average       |
|----------------|---------------|----------------|---------------|---------------|---------------|---------------|---------------|---------------|---------------|---------------|
| 14:00:00       | 0.220         | 561            | 0.995         | 0.985         | 0.990         | 0.985         | 0.965         | 0.970         | 0.925         | 0.974         |
| 15:00:00       | 0.217         | 531            | 0.930         | 0.965         | 0.980         | 0.965         | 0.960         | 0.965         | 0.930         | 0.956         |
| 16:00:00       | 0.218         | 438            | 0.920         | 0.935         | 0.960         | 0.950         | 0.940         | 0.945         | 0.905         | 0.936         |
| 17:00:00       | 0.212         | 313            | 0.905         | 0.925         | 0.940         | 0.940         | 0.930         | 0.935         | 0.895         | 0.924         |
| 18:00:00       | 0.211         | 331            | 0.920         | 0.940         | 0.950         | 0.950         | 0.940         | 0.940         | 0.895         | 0.934         |
| 19:00:00       | 0.212         | 282            | 0.910         | 0.945         | 0.950         | 0.950         | 0.940         | 0.940         | 0.890         | 0.932         |
| 20:00:00       | 0.218         | 279            | 0.915         | 0.950         | 0.955         | 0.940         | 0.935         | 0.930         | 0.880         | 0.929         |
| 21:00:00       | 0.204         | 459            | 1.000         | 1.000         | 0.980         | 0.945         | 0.950         | 0.940         | 0.865         | 0.954         |
| <b>Average</b> | <b>0.2140</b> | <b>399.250</b> | <b>0.9369</b> | <b>0.9556</b> | <b>0.9631</b> | <b>0.9531</b> | <b>0.9450</b> | <b>0.9456</b> | <b>0.8981</b> | <b>0.9424</b> |

Table 9. Correlation values at the seven wavelengths between both black carbon and SSA, and between the AOD and SSA.

| Wavelength nm  | Black Carbon Correlation | AOD Correlation |
|----------------|--------------------------|-----------------|
| 300            | 0.029                    | 0.594           |
| 305            | 0.021                    | 0.546           |
| 311            | -0.07                    | 0.439           |
| 317            | -0.05                    | 0.546           |
| 325            | -0.06                    | 0.554           |
| 332            | -0.03                    | 0.617           |
| 368            | -0.04                    | 0.689           |
| <b>Average</b> | <b>-0.028</b>            | <b>0.5915</b>   |

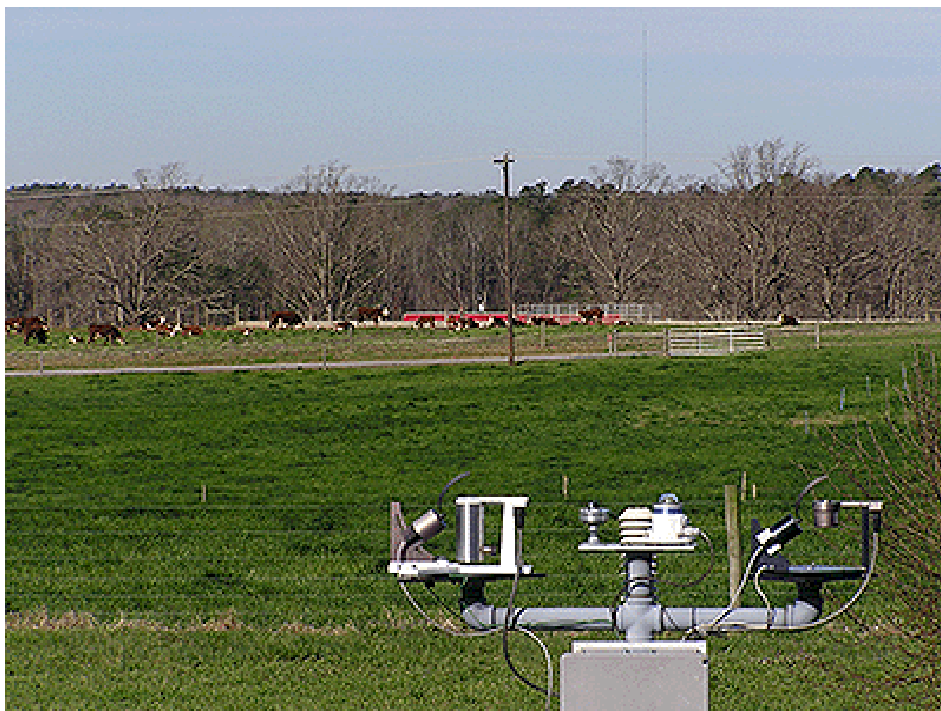


Figure 1. Picture of the UVMFR-SR instrument used to collect ultraviolet irradiances at the USDA's Lake Wheeler site about six miles south of Raleigh, NC.

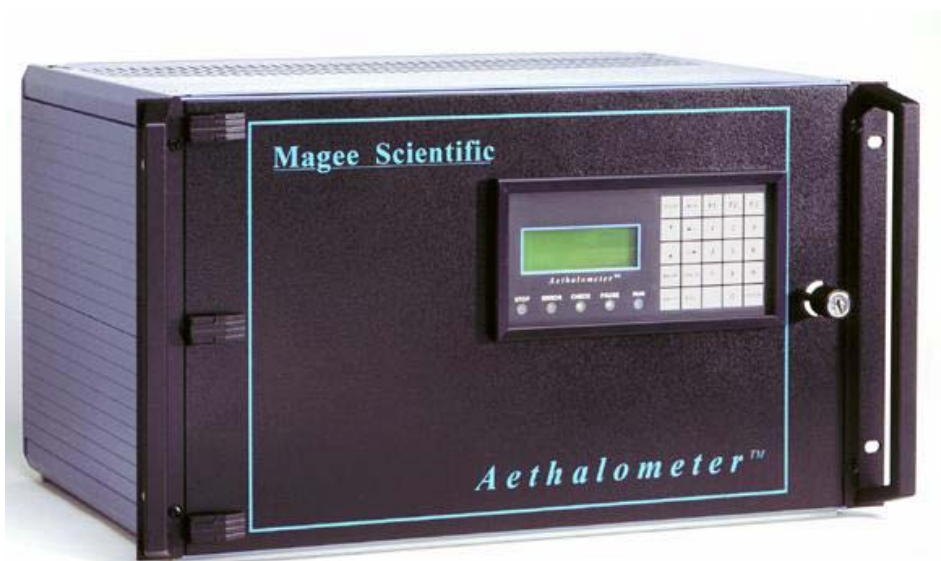


Figure 2. Picture of the Magee Scientific Aethalometer used to measure the black carbon concentrations at Lake Wheeler.

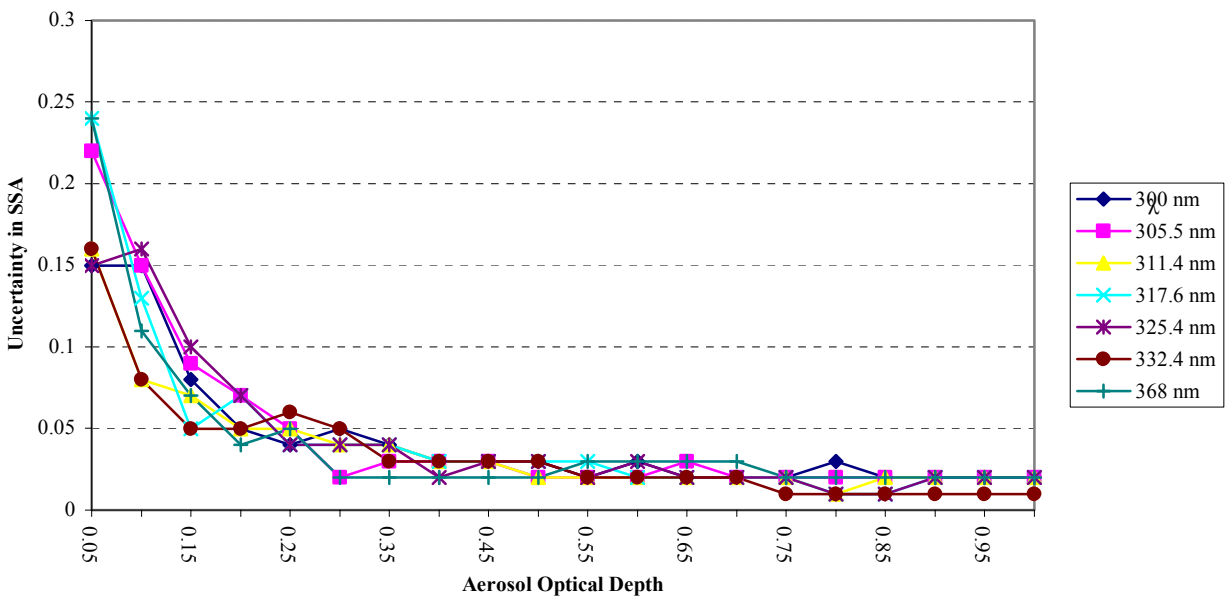


Figure 3. Estimated uncertainty in single scattering albedo (SSA) as functions of wavelength ( $\lambda$ ) and aerosol optical depth (AOD). This graph is from *Peters et al.*, 2003.

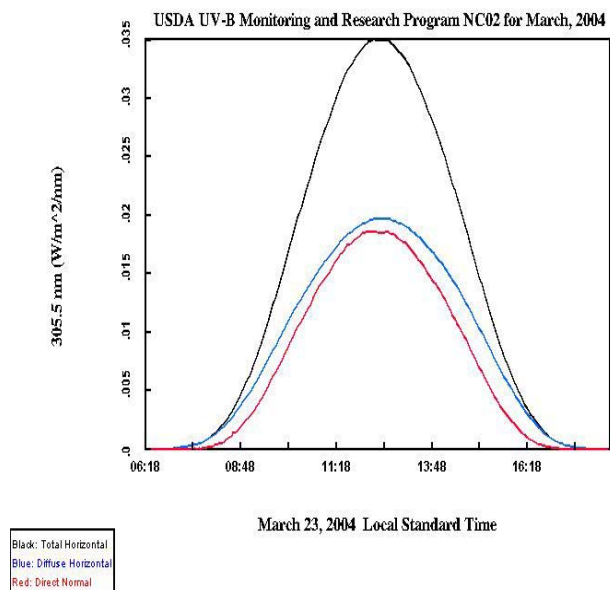


Figure 4. A plot of total UV irradiance (black line), direct irradiance (red line), and diffuse irradiance (blue line) at 305.5 nm on March 23, 2004 at Lake Wheeler. The smooth bell curves are indicative of a completely clear day at the site.

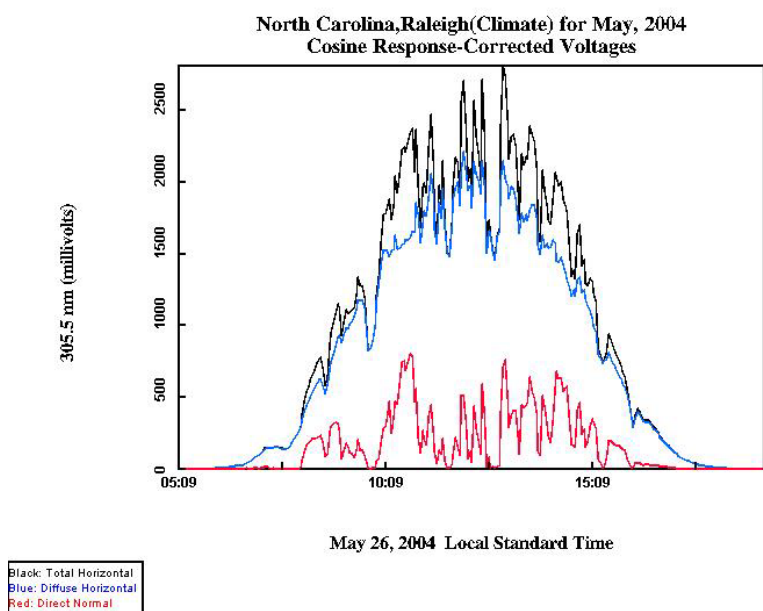


Figure 5. Same type of data as shown in figure 2, but with considerable clouds throughout the day. This day would not have been suitable for single scattering albedo retrieval. This graph shows the UV data for May 24, 2004.

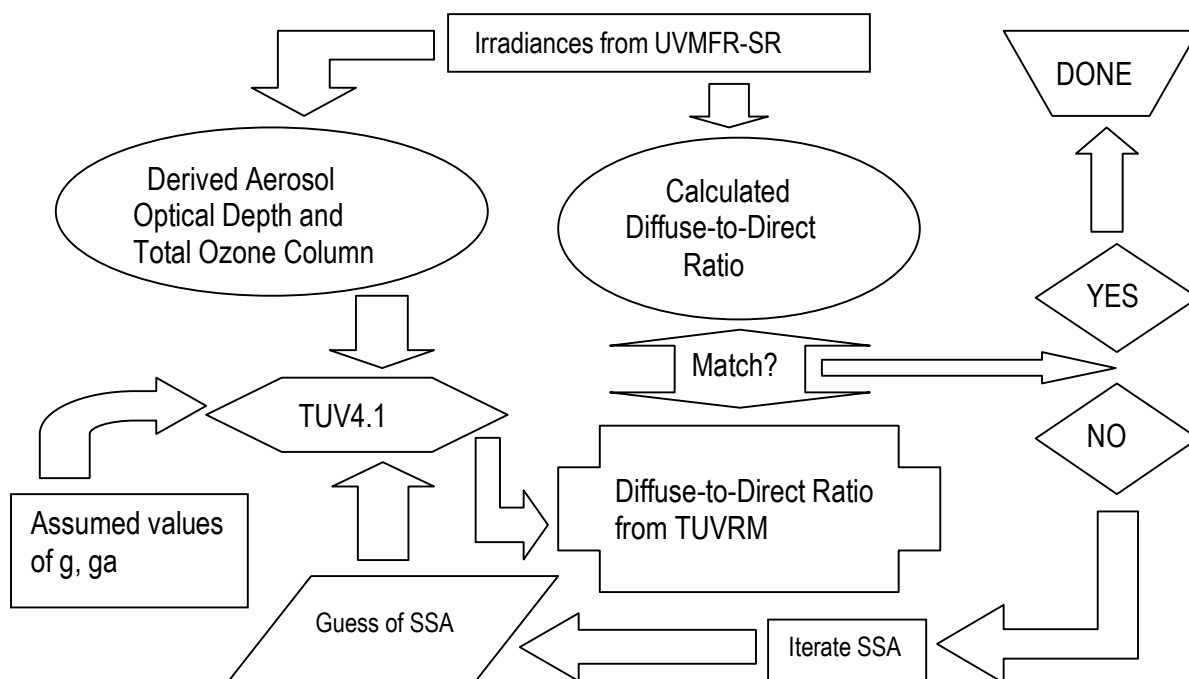


Figure 6. Diagram outlining the inversion process of single scattering albedo (SSA) retrieval. Adopted from *Petters et al., 2003*.

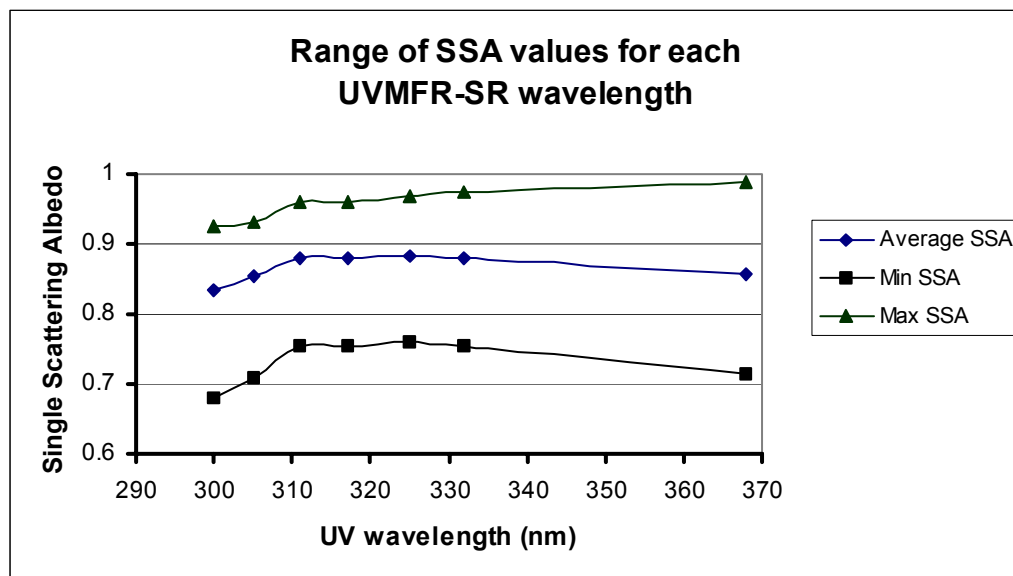


Figure 7. Average single scattering albedo for each UVMFR-SR wavelength, along with the range of these values, for the entire study period at the 45-degree solar zenith angle.

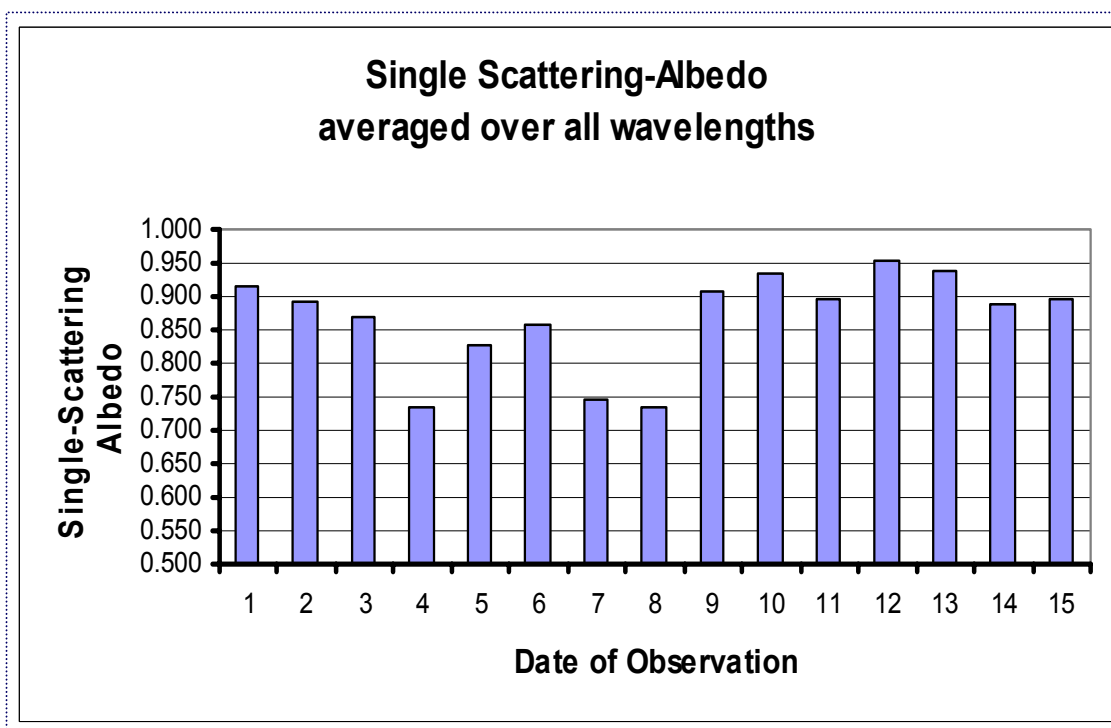


Figure 8. Bar graph showing the average single scattering albedo over all seven UVMFR-SR wavelengths for each day in this study.

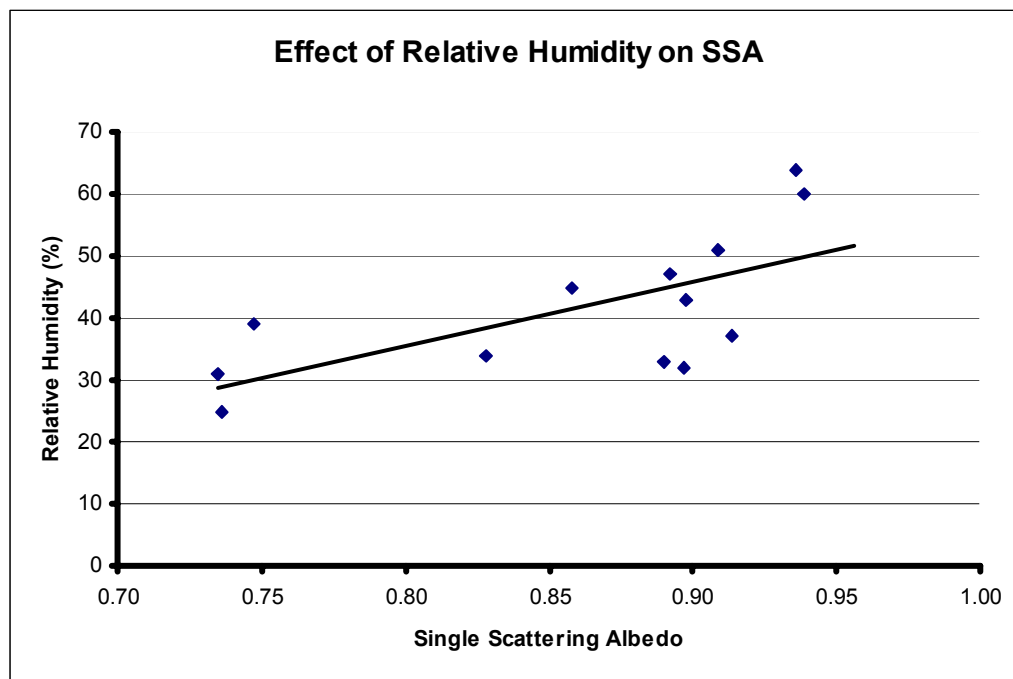


Figure 9. Scatter plot of relative humidity measured at Lake Wheeler as a function of the single scattering albedo. A linear regression line was applied to this data.

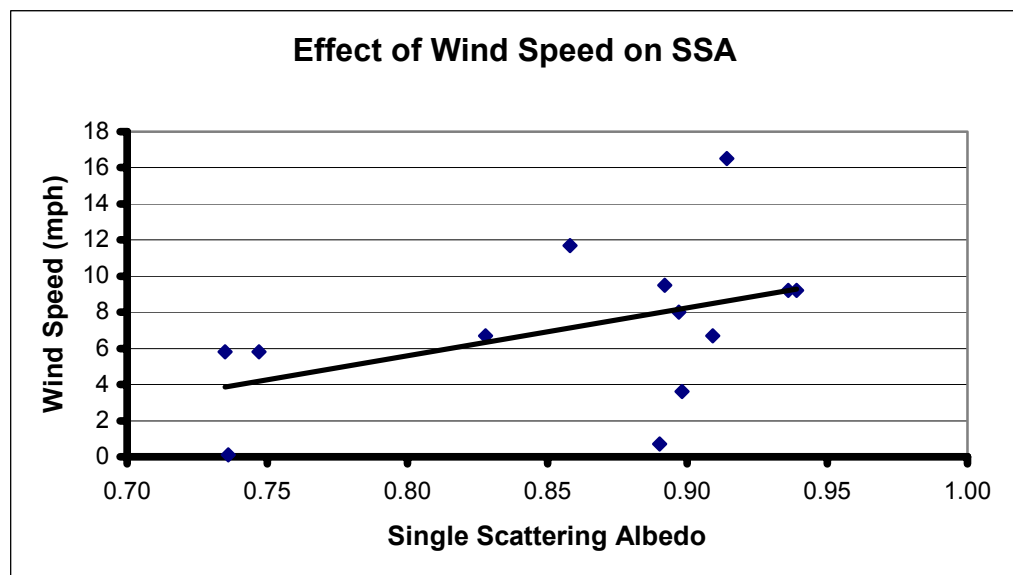


Figure 10. Scatter plot of wind speed measured at Lake Wheeler as a function of the single scattering albedo. A linear regression line was applied to this data.

## 5. Future Work

As of the time this research project was completed, little research has been devoted to studying aerosol single-scattering albedo in the ultraviolet wavelengths, and much more needs to be done in order to fully understand how aerosols attenuate UV radiation reaching the earth's surface. As single-scattering albedo plays an important role in reducing UV radiation at the surface, information concerning its value would prove most useful.

The values of SSA found in this study are in the spring, summer and early autumn months of 2004 only. Long-term UVMFR-SR measurements will allow for investigation of both seasonal and annual variation of single-scattering albedo. In addition, more locations for SSA research will give a better overall picture of areas where either absorption or reflection of radiation by aerosols may be occurring. Obtaining in-situ airborne measurements of single scattering albedo through scattering and absorption coefficients would also be helpful in studying this phenomenon. This would yield better spatial resolution.

A method has recently been devised to identify clear-sky periods using downwelling total and diffuse irradiance measurements such as those from the UVMFR-SR [Long and Ackerman, 2000]. This procedure is more sophisticated than the human observation procedure used in the current study, as well as the Petters and Wenny studies. The new method described by Long and Ackermann could theoretically be utilized with the current methodology to allow for determination of single scattering albedo on days when there are some clouds in the sky, but not enough clouds to prevent clear-sky periods during the day. Completely cloud-free days are relatively uncommon and much more data can be obtained for days when partly cloudy conditions are present. Aerosol optical depth could be extrapolated from irradiance measurements made during only the clear-sky

periods and subsequently used as input into the TUV model. This could allow for a wider database of single scattering albedo values from the database to be used in studies similar to this one.

## 6. Summary

The objective of this paper was to determine aerosol optical properties in the ultraviolet spectrum and their relationship to black carbon concentrations and aerosol optical depth measurements from the USDA's Lake Wheeler site near Raleigh, North Carolina. Aerosol single scattering albedo (SSA) was retrieved at the 45-degree morning solar zenith angle for 15 days from March to September of 2004 at the seven operational wavelengths of the UVMFR-SR. The results ranged from 0.680 to 0.990 and varied quadratically with increasing wavelength. This range of SSA was within the range of previous studies. The overall average SSA for this study was 0.867, indicating that most of the UV radiation incident to the particles is scattered, rather than absorbed. This reduces the direct UV irradiance by increasing the diffuse component. In addition, two of these days were selected for hourly retrievals of SSA and it was found that the minimum amount of scattering of UV radiation by aerosols occurred near solar noon. More scattering occurred earlier in the morning and later in the afternoon.

When the data were compared to the black carbon levels measured at Lake Wheeler, only a weak negative correlation was determined, indicating that a high concentration of black carbon had a limited role in reducing the SSA. Other suspended particulate matter, including fine dust and sea salt particles, may have played a larger role in the SSA as compared to the black carbon particulates alone. In contrast, there was a stronger positive correlation between aerosol optical depth and SSA, meaning more scattering with higher levels of aerosols. There was also a significant positive correlation between the relative humidity and SSA. The values of SSA found here can be used for better estimation of this parameter in these wavelengths for the southeastern United States.

This research is important in understanding the relationship between suspended particulate matter in the atmosphere and the transmission of harmful UV radiation. The limited research in this area has not given environmental scientists enough information to draw strong conclusions about how much aerosols affect UV radiation reaching the surface. It is important to ascertain how much of the global UV irradiance is actually being blocked from reaching the surface by aerosol particles, and whether this is indeed masking the serious nature of ozone depletion in the stratosphere by CFC's and other ozone-destroying compounds. Based on research performed thus far, if our atmosphere was totally void of any aerosol particles, it is safe to assume that the level of harmful UV radiation would be considerably higher. The main issue is to ascertain the extent to which this phenomenon of UV scattering by aerosols is occurring. Knowing this information will prove helpful in future modeling studies of aerosols by being able to provide more model inputs that can better predict atmosphere-aerosol interactions. An important benefit of improved modeling is a better understanding of how aerosols can reduce surface UV irradiances and thus reduce the negative biological consequences of UV radiation exposure.

## 7. References

- Bahrman, C. P., and V. K. Saxena, Influence of air mass history on black carbon concentrations and regional climate forcing in southeastern United States, *J. Geophys. Res.*, *103*, 23153-23161, 1998.
- Barnard, W. F., V.K. Saxena, B. N. Wenny, and J. J. DeLuisi, Daily surface UV exposure and its relationship to surface pollutant measurements, *J. Air Waste Management Assoc.*, 237-245, 2003.
- Bauman, W., UVMFR-7 UV Multi-Filter Rotating Shadow Band Radiometer. April 17, 2002, Yankee Environmental Systems. May 7, 2002, <<http://www.yesinc.com/products/data/uvmfr7/index.html>>.
- Blumthaler, M., and W. Ambach, Solar UVB-albedo of various surfaces, *Photochem. Photobiol.*, *48*, 85-88, 1988.
- Bidigare, R. R., Potential effects of UV-B radiation on marine organisms of the southern ocean: Distribution of phytoplankton and krill during austral spring, *Photochem. Photobiol.*, *50*, 469-477, 1989.
- Bigelow, D. S., J. R. Slusser, A. F. Beaubien, and J. H. Gibson, The USDA Ultraviolet Radiation Monitoring Program, *Bull. American Meteorological Soc.*, *79*, 601-615, 1998.
- Bojkov, R. D., and V. E. Fioletov, Estimating the global ozone characteristics during the last 30 years, *J. Geophys. Res.*, *100*, 16537-16551, 1995.
- Caldwell, M. M., C. W. Camp, C. W. Warner, and S. D. Flint, Action spectra and their key role in assessing biological consequences of solar UV-B radiation change, *Stratospheric Ozone Reduction, Solar Ultraviolet Radiation and Plant Life*, R.C. Worrest and M.M. Caldwell, Eds., Springer-Verlag, 87-111, 1986.
- Charlson, R. J., A. H. Vanderpol, D. S. Covert, A. P. Waggoner, and N. C. Ahlquist, H<sub>2</sub>SO<sub>4</sub>/(NH<sub>4</sub>)<sub>2</sub>SO<sub>4</sub> aerosol, optical detection in St. Louis region, *Atmos. Environ.*, *8*, 1257, 1974.
- Damkaer, D. M., D. B. Dey, and G. A. Heron, Dose/dose-rate responses of shrimp larvae to UV-B radiation, *Oecologia*, *48*, 178-182, 1981.
- Deininger, C. K., and V. K. Saxena, A validation of back trajectories of air masses by principal component analysis of ion concentrations in cloud water, *Atmos. Environ.*, *23*, 295-300, 1997.
- Diffey, B. L., A. T. Green, M. J. Loftus, G. J. Johnson, and P. S. Lee, A portable instrument for measuring ground reflectance in the ultraviolet, *Photochem. Photobiol.*, *61*, 68-70, 1995.
- Elterman, L. UV, visible, and IR attenuation for altitudes to 50 km, *AFCRL Rep.*, *AFCRL-68-0153, Environ. Res. Pap.* 285, 49 pp. Air Force Cambridge Res. Lab., Hanscom Air Force Base, Mass., 1968.

- Farman, J. C., B. G. Gardiner, and J. D. Shanklin, Large losses of total ozone in Antarctica reveal seasonal ClO<sub>x</sub>/NO<sub>x</sub> interaction, *Nature*, 315, 207-210, 1985.
- Frederick, J. E., E. K. Koob, A. D. Alberts, and E. C. Weatherhead, Empirical studies of tropospheric transmission in the ultraviolet: Broadband measurements, *J. Appl. Meteorol.*, 32, 1883-1892, 1993.
- Gundel, L. A., R. L. Dod, H. Rosen, and T. Novakov, The relationship between optical attenuation and black carbon concentration for ambient and source particles, *Sci. Total Environ.*, 36, 197-202, 1984.
- Hansen, A. D. A., *Magee Scientific Aethalometer User's Guide*, 56 pp., Magee Scientific Company, Berkeley, California, 1996.
- Hansen, J., M. Sato, and R. Ruedy, Radiative forcing and climate response, *J. Geophys. Res.*, 102, 6831-6864, 1997.
- Harrison, L., and J. Michalsky, Objective algorithms for the retrieval of optical depths from ground-based measurements, *Appl. Opt.*, 33, 5126-5132, 1994.
- Harrison, L., J. Michalsky, and J. Berndt, Automated multifilter rotating shadow-band radiometer: An instrument for optical depth and radiation measurements, *Appl. Opt.*, 33, 5118-5125, 1994.
- Im, J.-S., V. K. Saxena, and B. N. Wenny, Temporal trends of black carbon concentrations and regional climate forcing in the southeastern United States, *Atmos. Environ.*, 35, 3293-3302, 2001.
- Japar, S. M., W. W. Brachaczek, R. A. Gorse, J. M. Norbeck, and W. R. Pierson, The contribution of elemental carbon into the optical properties of rural atmospheric aerosols, *Atmos. Environ.*, 20, 1281-1289, 1986.
- Kerr, J. B., and C. T. McElroy, Evidence for large upward trends of ultraviolet-B radiation linked to ozone depletion, *Science*, 262, 1032-1034, 1993.
- Komhyr, W. D., Operations handbook—ozone observations with a Dobson spectrophotometer. WMO Global Ozone Research and Monitoring Project Rep. 6, *World Meteorological Organization*, Geneva, Switzerland, 1980.
- Krotkov, N. A., P. K. Bhartia, J. R. Herman, V. Fioletov, and J. Kerr, Satellite estimation of spectral surface UV irradiance in the presence of tropospheric aerosols, *J. Geophys. Res.*, 103, 8779-8793, 1998.
- Krzyscin, J.W., and S. Puchalski, Aerosol impact on the surface UV radiation from the ground-based measurements taken at Belsk, Poland, 1980-1996, *J. Geophys. Res.*, 103, 16175-16181, 1998.

Kylling, A., A. F. Bais, M. Blumthaler, J. Schreder, C. S. Zerefos, and E. Kosmidis, Effect of aerosols on solar UV irradiances during the Photochemical Activity and Solar Ultraviolet Radiation campaign, *J. Geophys. Res.*, *103*, 26,051-26,060, 1998.

Kylling, A. T. Persen, B. Mayer, and T. Svenøe, Determination of an effective spectral surface albedo from ground-based global and direct UV irradiance measurements, *J. Geophys. Res.*, *105*, 4949-4959, 2000.

Lacis, A. A., and M. I. Mishchenko, Climate forcing, cloud sensitivity, and climate response: A radiative modeling perspective on atmospheric aerosols, in *Aerosol Forcing of Climate*, edited by R. J. Charlson and J. Heintzenberg, pp. 11-40, John Wiley, New York, 1995.

Leffell, D. J., and D. E. Brash, *Sunlight and Skin Cancer*, pp. 52-59, Sci. Am., New York, 1996.

Liousse, C., H. Cachier, and S. G. Jennings, Optical and thermal measurements of black carbon aerosol content in different environments: variation of the specific attenuation cross-section, *Atmos. Environ.*, *27A*, 1203-1211, 1993.

Liu, S. C., S. A. McKeen, and S. Madronich, Effect of anthropogenic aerosols on biologically active ultraviolet radiation, *Geophys. Res. Lett.*, *18*, 2265-2268, 1991.

Long, C. S., A. J. Miller, H.-T. Lee, J. D. Wild, R. C. Przywarty, and D. Hufford. Ultraviolet index forecasts issued by the National Weather Service, *Bull. American Meteorological Soc.*, *77*, 729-748, 1996.

Long, C. N., and T. P. Ackerman, Identification of clear skies from broadband pyranometer measurements and calculation of downwelling shortwave cloud effects, *J. Geophys. Res.*, *105*, 15609-15626, 2000.

Lorente, J., A. Redano, and X. D. Cabo, Influence of urban aerosol on spectral solar irradiance, *J. Applied Meteorology*, *33*, 406-414, 1994.

Madronich, S., *Environmental Effects of Ultraviolet(UV) Radiation*, chapter: UV radiation in the natural and perturbed atmosphere, Lewis Publisher, Boca Raton, pp. 17-69, 1993.

TUV4.1 (Tropospheric Ultraviolet & Visible) Radiation Model, 2001. Web address: <http://www.acd.ucar.edu/TUV/>, UCAR Atmospheric Chemistry Division, Boulder, CO.

Madronich, S., and S. Flocke, Theoretical estimation of biologically effective UV radiation at the earth's surface, in *Solar Ultraviolet Radiation*, edited by C.S. Zerefos and A.F. Bais, Springer-Verlag, Berlin, 1997.

Madronich, S., R. L. McKenzie, L. O. Björn, and M. M. Caldwell, Changes in biologically active ultraviolet radiation reaching the Earth's surface, *Photochem. Photobiol.*, *46*, 5-19, 1998.

Malm, W. C., *Introduction to Visibility*, Air Resources Division, National Park Service, Cooperative Institute for Research in the Atmosphere (CIRA), NPS Visibility Program, Colorado State University, Fort Collins, CO, May 1999.

McInnes, L. M., M. H. Bergin, J. A. Ogren, and S. E. Schwartz, Apportionment of light scattering and hygroscopic growth to aerosol composition, *Geophys. Res. Lett.*, *25*, 513-516, 1998.

Meleti, C., and F. Cappellani, Measurements of aerosol optical depth at Ispra: Analysis of the correlation with UV-B, UV-A, and total solar irradiance, *J. Geophys. Res.*, *105*, 4971-4978, 2000.

Morison, W. L., Effects of ultraviolet radiation on the immune system in humans, *Photochem. Photobiol.*, *50*, 515-524, 1989.

Ogren, J. A., and R. J. Charlson, Elemental carbon in the atmosphere: cycle and lifetime, *Tellus*, *35-B*, 241-254, 1983.

Petters, J. L., V. K. Saxena, J. R. Slusser, B. N. Wenny, and S. Madronich, Aerosol single scattering albedo retrieved from measurements of surface UV irradiance and a radiative transfer model, *J. Geophys. Res.*, *108*(D9), 2003.

Pitari, G., E. Mancini, V. Rizi, and D. T. Shindell, Impact of future climate and emission changes on stratospheric aerosols and ozone, *J. Atmos. Sci.*, *59*, 414-440, 2002.

Reuder, J., and H. Schwander, Aerosol effects on UV radiation in nonurban regions, *J. Geophys. Res.*, *104*, 4065-4077, 1999.

Rood, M. J., D. S. Covert, and T. V. Larson, Hygroscopic properties of atmospheric aerosol in Riverside, California, *Tellus*, Ser. B., *39*, 383-397, 1987.

Russak, V., Atmospheric aerosol variability in Estonia calculated from solar radiation measurements, *Tellus*, *48A*, 786-791, 1996.

Schafer, J. S., V. K. Saxena, B. N. Wenny, W. Barnard, and J. J. DeLuisi, Observed influence of clouds on ultraviolet-B radiation, *Geophys. Res. Lett.*, *23*, 2625-2628, 1996.

Schwander, H., P. Koepke, and A. Ruggaber, Uncertainties in modeled UV irradiances due to limited accuracy and availability of input data, *J. Geophys. Res.*, *102*, 9419-9429, 1997.

Stanhill, G., and A. Janetz, Long-term trends in, and the spatial variability of, global irradiance in Israel, *Tellus*, *49B*, 112-122, 1997.

Stolarski, R. S., R. D. McPeters, and P. A. Newman, The ozone hole of 2002 as measured by TOMS, *J. Atmos. Sci.*, *62*, 716-720, 2003.

- Tang, I. N., Deliquescence properties and particle size change of hygroscopic aerosols, in *Generation of Aerosols and Facilities for Exposure Experiments*, ed. K. Willeke, Ann Arbor Science, Ann Arbor, MI., 1980.
- Taylor, H. R., The biological effects of UV-B on the eye, *Photochem. Photobiol.*, *50*, 489-492, 1989.
- Tevini, M., and A. H. Teramura, UV-B effects on terrestrial plants, *Photochem. Photobiol.*, *50*, 479-487, 1989.
- Waggoner, A. P., R. E. Weiss, N. C. Ahlquist, D. S. Covert, S. Will, and R. J. Charlson, Optical characteristics of atmospheric aerosols, *Atmos. Environ.*, *15*, 1891-1909, 1981.
- Weihs, P., A. R. Webb, S. J. Hutchinson, and G. W. Middleton, Measurements of the diffuse UV sky radiance during broken cloud conditions, *J. Geophys. Res.*, *105*, 4937-4944, 2000.
- Wenny, B. N., V. K. Saxena, and J. E. Frederick, Aerosol optical depth measurements and their impact on surface levels of ultraviolet-B radiation, *J. Geophys. Res.*, *106*, 17311-17319, 2001.
- Wenny, B. N., J. S. Schafer, J. J. DeLuisi, V. K. Saxena, W. F. Barnard, I. V. Petropavlovskikh, and A. J. Vergamini, A study of regional aerosol radiative properties and effects on ultraviolet-B radiation, *J. Geophys. Res.*, *103*, 17,083-17,097, 1998.
- Worrest, R. C., K. D. Smythe, and A. M. Tait, Linkages between climate change and stratospheric ozone depletion, *Global Climate Change Linkages, Acid Rain, Air Quality and Stratospheric Ozone*, J. C. White, Ed., Elsevier Science, 67-78, 1989.
- Yu, S., V. K. Saxena, B. N. Wenny, J. J. DeLuisi, G. K. Yue, and I. V. Petropavlovskikh, A study of the aerosol radiative properties needed to compute direct aerosol forcing in the southeastern United States, *J. Geophys. Res.*, *105*, 24,739-24,749, 2000.